



Article

Integrative Transcriptome and Chlorophyll Fluorescence Test Analysis Shed New Light on the Leaf Senescence Mechanism of *Zoysia japonica*

Jin Guan ^{1,2}, Xifeng Fan ¹, Yuesen Yue ¹, Lixin Xu ² , Ke Teng ^{1,*}  and Shuxia Yin ^{2,*} 

¹ Institute of Grassland, Flowers, and Ecology, Beijing Academy of Agriculture and Forestry Sciences, Beijing 100097, China

² College of Grassland Science, Beijing Forestry University, Beijing 100083, China

* Correspondence: tengke@grass-env.com (K.T.); yinsx369@bjfu.edu.cn (S.Y.)

Abstract: *Zoysia japonica* is an important warm-season turfgrass used worldwide. The decreased aesthetic quality and functionality during leaf senescence hamper its further utilization. However, information about the transcriptional mechanism and genes involved in leaf senescence in *Z. japonica* needs to be more extensive. Therefore, to better understand leaf senescence in *Z. japonica*, we investigated the integrated analysis of chlorophyll fluorescence test (JIP-test) and RNA sequencing (RNA-seq) of mature and senescent leaves. First, we identified 22,049 genes, of which 4038 were differentially expressed genes (DEGs). The results for gene expression profiles were evaluated using quantitative real-time PCR. A total of 2515 genes have homologous genes in other plants. The matched known-function SAGs are mainly involved in chlorophyll degradation and plant hormone response. A total of 539 differentially expressed transcription factor genes, including AP2/ERF-ERF, NAC, WRKY, bHLH, and MYB, were identified to be associated with leaf senescence. Next, senescence represses chlorophyll biosynthesis while upregulating chlorophyll degradation. Senescence harms the integrity and functionality of PSII, PSI, and the intersystem electron transport chain. In addition, IAA biosynthesis was inhibited, whereas ABA and ET biosynthesis were activated in leaf senescence, and senescence activates signal transduction of IAA, ABA, and ET. These findings add to our understanding of the regulatory mechanism of leaf senescence. The senescence-associated genes are candidate targets for providing new insight into leaf senescence modeling in *Z. japonica*. They provided a theoretical foundation to reveal the functions of senescence-associated genes and chlorophyll catabolic genes involved in leaf senescence.

Keywords: *Zoysia japonica*; leaf senescence; RNA sequencing; chlorophyll fluorescence; plant hormones



Citation: Guan, J.; Fan, X.; Yue, Y.; Xu, L.; Teng, K.; Yin, S. Integrative Transcriptome and Chlorophyll Fluorescence Test Analysis Shed New Light on the Leaf Senescence Mechanism of *Zoysia japonica*. *Agronomy* **2023**, *13*, 623. <https://doi.org/10.3390/agronomy13030623>

Academic Editors: Wanjun Zhang and Jingjin Yu

Received: 25 December 2022

Revised: 9 February 2023

Accepted: 13 February 2023

Published: 22 February 2023



Copyright: © 2023 by the authors. Licensee MDPI, Basel, Switzerland. This article is an open access article distributed under the terms and conditions of the Creative Commons Attribution (CC BY) license (<https://creativecommons.org/licenses/by/4.0/>).

1. Introduction

As the final phase of plant development, leaf senescence constitutes a critical stage in the plant life cycle; it is not an uncontrolled and passive degeneration process [1,2]. The most observable symptom of leaf senescence is the de-greening driven by quick chlorophyll degradation during chloroplast degeneration [2]. Moreover, the degradation of proteins, carbohydrates, and other macromolecules and the mobilization of micronutrients occur in conjunction with leaf senescence [3,4]. However, leaf senescence may limit the utilization of ornamental plants and turfgrasses by causing leaf yellowing and an unaesthetic appearance [5]. Hence, understanding the molecular factors and regulatory mechanisms of leaf senescence enhances our insight into a fundamental biological process and provides the means to delay leaf senescence for genetic modification and molecular breeding.

The process of senescence-associated genes (SAGs) regulates leaf senescence in a highly systematic way [6]. SAGs in many plants, including *Arabidopsis thaliana*, *Zea mays*, and *Oryza sativa*, were identified and characterized recently to understand leaf senescence at the molecular level [7,8]. *SAG12*, *SAG13*, *SAG14*, and other SAGs are commonly accepted

senescence markers [9–11]. During leaf senescence, the expression of chlorophyll catabolic genes is under strict transcriptional regulation in perennial ryegrass (*Lolium perenne*) [12]. In addition, leaf senescence is tightly controlled and influenced by many transcription factors (TFs) [7,13]. Overexpression of an AP2 family transcription factor gene, *Rap2.4f*, promotes leaf senescence in *Arabidopsis* [14]. Abscisic acid (ABA) signals are integrated into leaf senescence by the *Arabidopsis* NAC transcription factor VNI2 through the *COR/RD* genes [15]. ORE1, an NAC transcription factor, is a positive senescence regulator and could activate the expression of senescence-associated genes and chlorophyll catabolic genes, such as *BFN1*, *SAG29*, *SINA1*, *NYE1*, *NYC1*, *PAO*, and *NOL* [16–18]. Moreover, ORE1 could promote the transcription of a significant ethylene biosynthesis gene, *ACS2*, and the forward regulation of ethylene (ET) biosynthesis and signal transduction [18]. Another NAC transcription factor, AtNAP, plays a critical role in leaf senescence [19]. AtNAP could bind with the promoter to induce the expression of the senescence-associated gene *SAG113* and mediate ABA-regulated leaf senescence [20]. A total of 23 WRKY genes showed increased transcription levels during leaf senescence in switchgrass [21]. MYBR1 was reported to be a negative regulator of ABA, stress, and wounding responses and a senescence inhibitor [22]. WRKY53 is a positive regulator, and WRKY54 and WRKY70 are negative regulators of leaf senescence [23,24]. WRKY53, WRKY54, and WRKY70 modulate leaf senescence by interacting with WRKY30 [24].

Recently, gene network analysis displayed that phytohormones are essential regulators of plant leaf senescence; altered hormone signaling causes many altered senescence phenotypes in *Arabidopsis* [25]. Hotspots for plant senescence are genes involved in plant hormone biosynthesis and signal transduction. Auxins (IAA) and cytokinin (CTK) play essential roles in all phases of plant development, from seed germination to senescence [26,27]. At present, the role of auxin in leaf senescence is controversial [28]. CTK negatively regulates leaf senescence [29,30]. Jasmonic acid (JA), salicylic acid (SA), ET, and ABA can promote plant senescence [3,10,31–33]. EIN3, a crucial positive regulator in ET signal transduction, could induce the expression of ORE1 to regulate senescence [18,34]. Moreover, EIN3, *miR164*, and ORE1 form a regulatory network that mediates leaf senescence [35,36]. The ABA receptor gene *PYL9* is essential for promoting leaf senescence and resistance to extreme drought stress in *Arabidopsis* [37]. In *Arabidopsis*, ABF2, ABF3, and ABF4 play crucial roles in regulating ABA-triggered chlorophyll degradation and leaf senescence [2].

Zoysia japonica ($2n = 4x = 40$) is a warm-season turfgrass with many excellent traits, including low maintenance and superior resistance to salinity, drought, and traffic [38–42]. However, the decreased aesthetic quality and functionality during leaf senescence hinder its further utilization in northern China [10,43]. Consequently, it is necessary to interpret the critical genes and regulatory mechanisms at the molecular level of leaf senescence in *Z. japonica*. The genome of *Z. japonica* was sequenced using the HiSeq and MiSeq platforms and published in 2016 [44]. In our previous report, we used the PacBio Sequel II platform to analyze the full-length transcriptome of *Z. japonica*. The sequencing data revealed 15,675 alternative splicing (AS) events and 5325 alternative polyadenylation (APA) sites, improving the reference genome [45]. The publication of genome and full-length transcriptome data provides essential information resources for the study of *Z. japonica*; nevertheless, previous studies on the transcriptional mechanism of leaf senescence in *Z. japonica* are limited. Moreover, how plant hormones, SAGs, and transcription factors function in leaf senescence in *Z. japonica* still needs to be explored.

Aiming to reveal the mechanism of leaf senescence in *Z. japonica*, an integrated analysis of RNA sequencing (RNA-seq) and chlorophyll fluorescence test (JIP-test) data was carried out. Senescence and photosynthesis-related genes, TFs, and critical regulatory components of the senescence process in *Z. japonica* were identified. These findings add to our understanding of the regulatory mechanism of leaf senescence and supply a theoretical foundation for the extended green period and the development of new cultivars of *Z. japonica*.

2. Materials and Methods

2.1. Plant Materials and Growth Conditions

We sowed *Z. japonica* seeds (cv. Zenith) purchased from Patten Seed Company (Lakeland, GA, USA) in Klasmann TS1 peat substrate (Klasmann-Deilmann, Geeste, Germany) and cultivated plants in a growth chamber with the temperature set at 28/25 °C (day/night), photosynthetic active radiation of 400 $\mu\text{mol m}^{-2} \text{s}^{-1}$ and a 14 h photoperiod per day. The potted plants were watered weekly and fertilized for two weeks with a Hoagland nutrition solution [46]. As described in our previous study [10], we collected mature and senescent leaves from the same lines of *Z. japonica* in September 2020. We selected three independent lines and used the RNA of each line for further experiments. The samples were frozen in liquid nitrogen and stored at -80 °C.

2.2. Chlorophyll, Soluble Sugar, and Plant Hormones Measurements

The content of chlorophyll and soluble sugar was determined using the previously published protocol [47]. Briefly, mature and senescent leaves (0.05–0.08 g) were harvested, weighed, and immersed in 8 mL 95% ethanol in the dark for 48 h. We obtained a plant soluble sugar content test kit (A145-2-1) from the Jiancheng Bioengineering Institute, Nanjing, China, to examine the content of soluble sugars in mature and senescent leaves. We purchased ELISA (H251) and ELISA (H602-1) kits from Nanjing Jiancheng Bioengineering Institute, Nanjing, China, to determine the ABA and IAA contents in mature and senescent leaves, respectively. All experiments in this study included at least three biological replicates.

2.3. Chlorophyll *a* Fluorescence Measurement and JIP-Test Parameters Analysis

We measured the prompt chlorophyll fluorescence after a 30 min dark adaptation using a Handy PEA Plant efficiency analyzer (Hansatech, Kings Lynn, U.K.). As described in our previous study [47], the measuring protocol included 2 s saturation light pulses with a light intensity of 3500 $\mu\text{mol photons m}^{-2} \text{s}^{-1}$. Eleven replicants of mature and senescent leaves were used for chlorophyll fluorescence transient recording. Average values of induction curves and standard errors in the same group were calculated from all the investigated objects.

2.4. Illumina cDNA Library Construction and Sequencing

Total RNA was isolated from mature and senescent leaves of three different lines using a Plant RNA kit (Omega Bio-Tech, Norcross, GA, USA). RNA degradation and contamination were monitored on 1% agarose gels, and RNA concentration and purity were determined using the NANODROP 8000 (Thermo Fisher Scientific, Waltham, MA, USA). RNA integrity was evaluated using the Agilent 2100 (Agilent Technologies, Santa Clara, CA, USA). Following RNA extraction and quality assessment, 3 μg RNA per sample was used for Illumina library preparation. Six libraries (three biological replicates of mature and senescent leaves, respectively) were built and sequenced using the Illumina Novaseq6000 platform (San Diego, CA, USA) by Biomarker Technologies (Beijing, China). The GC content, Q20, and Q30 of clean data were calculated, and all downstream analyses relied on high-quality clean data.

2.5. Transcriptomic Analysis

We used HISAT2 [48] to align clean reads to the reference genome of *Z. japonica* [44] to obtain positional information on the reference genome or gene. The expression level of genes and read counts mapped to this gene were calculated using the fragments per kilobase of transcript per million fragments mapped (FPKM) method [49]. We used DESeq2 [50] to analyze differential expression after detecting correlations between bio-replicates using the Pearson correlation coefficient. The DEGs were identified using the criteria of a minimum fold change of 2 and an FDR of less than 0.01. The *p*-value was corrected via the Benjamini–Hochberg correction method. The DEGs were annotated and enriched using the workflow

of the Biomarker Cloud platform (www.biocloud.net, accessed on 3 February 2021). Data cleaning and visualization were accomplished using in-house Python and R scripts.

2.6. qRT-PCR Verification of DEGs

We collected mature and senescent leaves and isolated total RNA from each using a Plant RNA kit (Omega Bio-Tech, USA). We used PrimeScript™ Reverse Transcriptase (TaKaRa, Dalian, China) to perform reverse transcription and the Cycle Pure kit (OMEGA, Georgia, USA) to purify the product. We randomly selected ten DEGs for qRT-PCR verification. We used Primer Premier 6 software to design the primers.

qRT-PCR analysis was conducted on a Bio-Rad CFX Connect™ Real-Time System using SYBR® Premix Ex Taq™ II (TaKaRa, Dalian, China). The housekeeping gene was *Z. japonica* β -actin (GenBank accession No. GU290546). All gene expression analyses were performed using three biological replicates. The relative expression levels of genes were calculated using the $2^{-\Delta\Delta CT}$ method [42].

2.7. GO and Pathway Enrichment Analysis

We used GOrse R packages to implement GO enrichment analysis based on Wallenius non-central hypergeometric distribution, which adjusts for gene length bias in DEG [51]. As previously described, we used the KOBAS software (version 2.0) to test the statistical enrichment of DEGs in KEGG pathways [52].

3. Results

3.1. Physiological Changes and Hormone Levels Differences in Mature and Senescent Leaves

The leaves of *Z. japonica* began to enter senescence after growing for about four months, whereas other leaves remained green. We collected mature and senescent leaf samples for further experiments (Figure 1A). Chlorophyll and IAA levels decreased to 65.97% and 40.72% during leaf senescence progress, respectively, according to our measurements of their contents (Figure 1B,C). The soluble sugar content in senescent leaves elevated to 143.08% of mature leaves, while ABA increased to 190.14% (Figure 1D,E). The ratio of chlorophyll *a* (Chl *a*) to chlorophyll *b* (Chl *b*) is a necessary index to evaluate leaf senescence. In this study, the proportion of mature leaves to senescent leaves dropped to 49.32%, indicating accelerated senescent processes (Figure 1F). In conclusion, mature and senescent leaves were distinguished, which was supported by the levels of chlorophyll, IAA, soluble sugar, and ABA.

3.2. RNA-Seq Analysis of *Z. japonica* and the Identification of DEGs

The RNA of the harvested mature and senescent leaf samples was isolated, and six cDNA libraries (three biological replicates for mature and senescent leaves) were constructed. We processed these libraries using the Illumina NovaSeq6000 sequencing platform (San Diego, CA, USA). Each library produced between 23 and 26 million pair-end reads and clean data with high Q20 (>98%) and Q30 (>95%), ranging from 53.96% to 55.34% (Table 1). In the leaves of the two developmental stages, 22,049 genes (FPKM > 0) were identified (Table S1).

We discovered 4038 differentially expressed genes (DEGs) through DEG analysis, with 1851 upregulated genes and 2187 downregulated genes (Table S2). We randomly selected 10 genes (five upregulated and five downregulated genes) and designed primers (Table S3) for quantitative real-time PCR (qRT-PCR) verification. The DEGs analysis and the qRT-PCR results were comparable (Table 2), proving that RNA-seq was a reliable and accurate tool for determining the DEGs of *Z. japonica* leaf senescence.

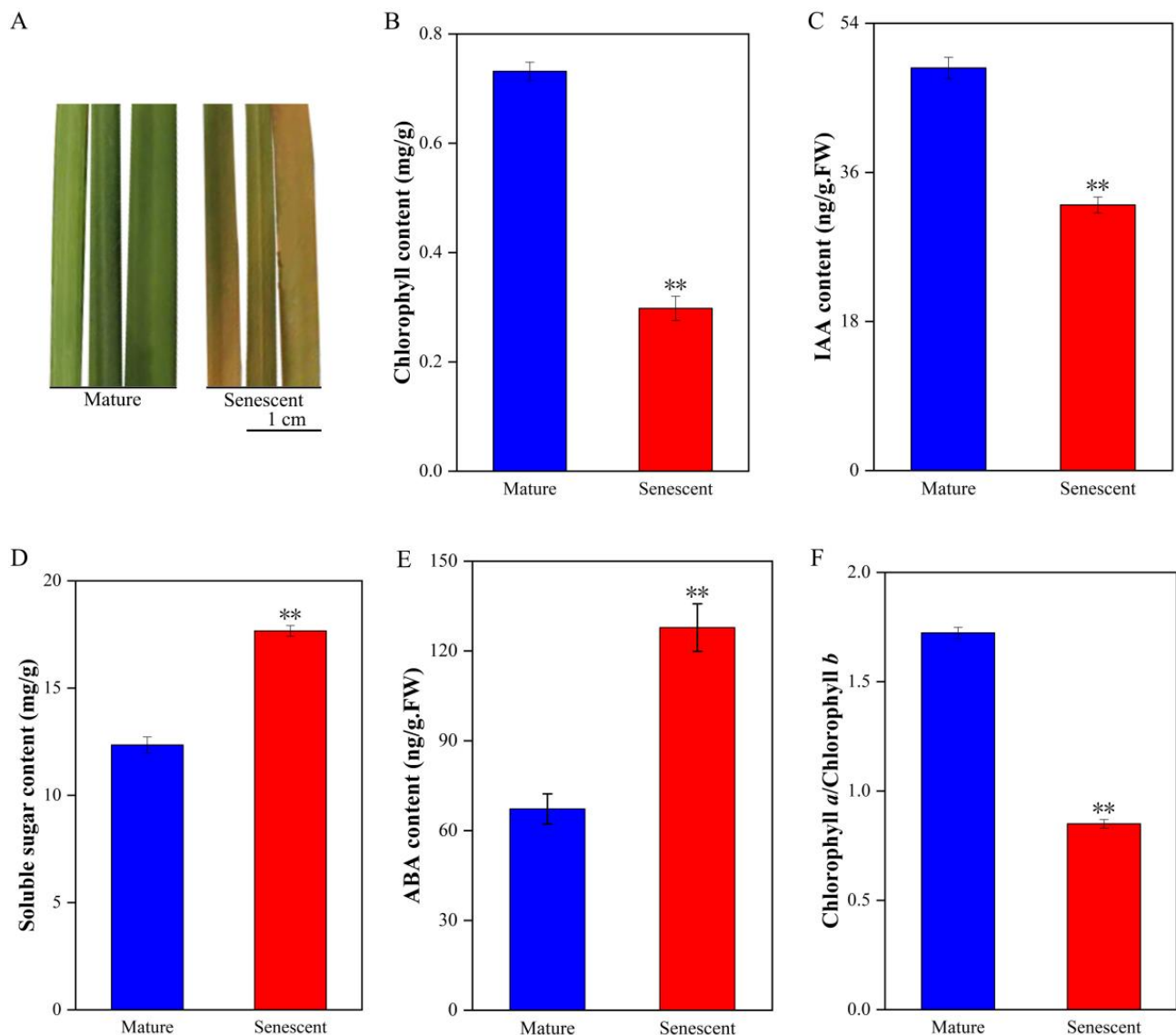


Figure 1. Phenotypes, physiology, and biochemical measurements. (A) Phenotypes of *Z. japonica* at mature and senescent stages. Chlorophyll (B), IAA (C), soluble sugar (D), and ABA (E) contents were measured in leaf samples at the mature and senescent stages. (F) The ratio of chlorophyll *a*/chlorophyll *b* was calculated in leaf samples at mature and senescent stages. Error bars represent the SD from three independent experiments. ** indicates significant differences in the means at $p < 0.01$ between mature and senescent leaves for each parameter measured ($n = 3$).

Table 1. Statistics on clean data quality evaluation of RNA-seq.

Sample Name	Read Sum	Base Sum	N (%)	GC (%)	Q20 (%)	Q30 (%)
Mature sample 1	24,158,349	7,199,286,172	0.00	55.06	98.45	95.69
Mature sample 2	22,712,448	6,766,266,766	0.00	55.34	98.30	95.30
Mature sample 3	24,681,745	7,352,597,992	0.00	55.03	98.42	95.57
Senescent sample 1	24,651,354	7,368,053,620	0.00	54.66	98.34	95.36
Senescent sample 2	26,404,815	7,870,804,198	0.00	55.08	98.34	95.36
Senescent sample 3	23,812,657	7,122,890,816	0.00	53.96	98.24	95.03

Table 2. Verification of DEGs in mature and senescent leaves by qRT-PCR analysis.

Gene ID	Annotation	Regulated	Senescent/Mature (log ₂ FC)	
			Digital Expression	qRT-PCR
Zjn_sc03174.1.g00010.1.am.mk	Protein phosphatase 2C 64	up	1.74	1.16
Zjn_sc00001.1.g03760.1.sm.mkhc	Hypothetical protein TIFY 10B-like	up	2.19	2.12
Zjn_sc00003.1.g10610.1.sm.mkhc	Jasmonate ZIM domain protein, partial	up	1.97	2.03
Zjn_sc00059.1.g01300.1.sm.mk	Transcription factor MYC2	up	1.4	1.53
Zjn_sc00003.1.g01950.1.sm.mk	Ethylene insensitive 3-like 1 protein	up	1.86	1.12
Zjn_sc00138.1.g00080.1.am.mk	Cytochrome b6-f complex iron-sulfur subunit	down	−8.76	−2.42
Zjn_sc00184.1.g00360.1.am.mk	plastocyanin, chloroplastic-like	down	−5.18	−7.77
Zjn_sc00152.1.g00120.1.sm.mkhc	Ferredoxin–NADP reductase, leaf isozyme 2	down	−1.74	−3.39
PB.16272	photosystem II protein D2	down	−1.97	−2.07
PB.4217	ATP synthase CF1 alpha subunit	down	−3.20	−0.87

3.3. SAG Conservation Analyses

We compared the 4038 DEGs with the Leaf Senescence Database (LSD 4.0, <http://ngdc.cnca.ac.cn/lsc/>, accessed on 9 September 2022) to evaluate SAG orthologs between *Z. japonica* and other plants. A total of 2515 (62.3%) DEGs have homologous genes in other plants. Based on the function and classification of their most closely related homolog, 2515 genes were divided into several categories, mainly participating in transcriptional regulation, plant hormone responses, chlorophyll degradation, and lipid/carbohydrate metabolism (Table S4).

3.4. GO and KEGG Analysis

Using the GO database, we annotated 3117 differentially expressed genes (DEGs) into three categories. Genes in biological processes mainly consist of metabolic, cellular, and single-organism processes. For the cellular component category, genes were enriched for membrane, cell, cell part, membrane part, and organelle. For the molecular function category, genes were mainly involved in binding and catalytic activity. More details are shown in Table S5.

We annotated 2474 DEGs using the KEGG database. The KEGG annotations were analyzed and classified to identify metabolic pathways. The KEGG results demonstrated 117 KEGG pathways mapped to 1137 upregulated genes, while 120 KEGG pathways mapped to 1337 downregulated genes (Tables S6 and S7). There were three upregulated and 11 downregulated pathways with corrected *q*-value < 0.05 in the senescent leaf of *Z. japonica* (Table 3). The results showed that “autophagy-other”, “ether lipid metabolism”, and “phenylpropanoid biosynthesis” were activated. The pathways involved in “photosynthesis-antenna proteins”, “carbon fixation in photosynthetic organisms”, “photosynthesis”, “ribosome”, “porphyrin and chlorophyll metabolism”, “carbon metabolism”, “carotenoid biosynthesis”, “pentose phosphate pathway”, “glycolysis/gluconeogenesis”, “ubiquinone and other terpenoid-quinone biosynthesis”, and “fructose and mannose metabolism” were withheld (Table 3).

3.5. Transcription Factor Analysis

TFs are essential regulatory proteins that control leaf senescence. A total of 539 TFs from 117 TF families were identified (Table S8), and the top 12 families are shown in Figure 2. The top seven TF families were AP2/ERF-ERF (34), NAC (33), Others (29), WRKY (26), bHLH (25), MYB (21), bZIP (19). A total of 293 transcription factors, including 27 NAC, 14 MYB, 13 AP2/ERF-ERF, 13 bHLH, and 13 WRKY proteins, were sig-

nificantly upregulated in senescent leaves. The genes *Zjn_sc00033.1.g00990.1.am.mkhc* and *Zjn_sc00205.1.g00380.1.sm.mkhc*, encoding AP2/ERF-ERF proteins, showed more than a 10-fold increase in the level of expression. The bHLH transcription factor gene (*Zjn_sc00022.1.g00530.1.sm.mkhc*) and the MYB-related transcription factor gene (*Zjn_sc00087.1.g00290.1.am.mk*) were upregulated more than 17-fold in senescent leaves. Moreover, 246 TFs, including 21 AP2/ERF-ERF proteins, were significantly downregulated during leaf senescence. The gene *Zjn_sc00022.1.g04840.1.sm.mk*, encoding bHLH protein, was reduced to less than 1/100 times in senescent leaves. An HB-HD-ZIP transcription factor gene, *Zjn_sc00004.1.g06420.1.sm.mkhc*, was decreased to less than 1/180 times in senescent leaves.

Table 3. Significantly enriched pathways in *Z. japonica* during leaf senescence.

Kegg_Pathway	ko_id	Input Number	Corrected_ <i>q</i> -Value	Up- or Downregulated
Autophagy—other	ko04136	14	0.000200076	Upregulated
Ether lipid metabolism	ko00565	11	0.004112946	Upregulated
Phenylpropanoid biosynthesis	ko00940	40	0.015142676	Upregulated
Photosynthesis-antenna proteins	ko00196	22	8.09×10^{-19}	Downregulated
Carbon fixation in photosynthetic organisms	ko00710	46	1.27×10^{-11}	Downregulated
Photosynthesis	ko00195	49	8.94×10^{-11}	Downregulated
Ribosome	ko03010	61	8.21×10^{-6}	Downregulated
Porphyrin and chlorophyll metabolism	ko00860	21	1.89×10^{-5}	Downregulated
Carbon metabolism	ko01200	61	3.81×10^{-5}	Downregulated
Carotenoid biosynthesis	ko00906	16	0.007050826	Downregulated
Pentose phosphate pathway	ko00030	18	0.017326576	Downregulated
Glycolysis/gluconeogenesis	ko00010	34	0.019536307	Downregulated
Ubiquinone and other terpenoid-quinone biosynthesis	ko00130	13	0.16294735	Downregulated
Fructose and mannose metabolism	ko00051	18	0.259466752	Downregulated

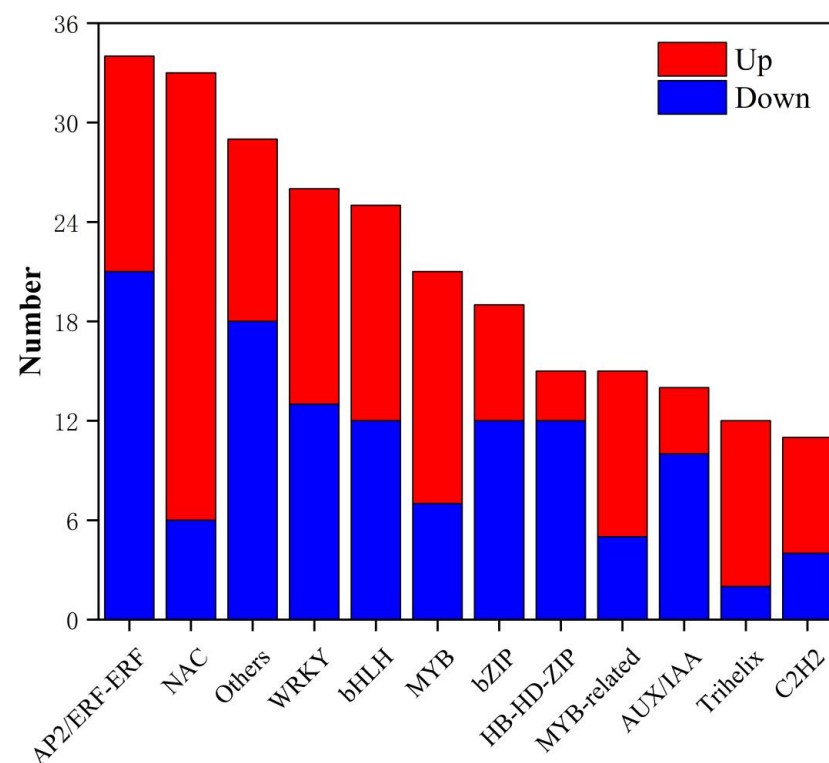


Figure 2. Differentially expressed transcription factor genes in leaf senescence. The *x*-axis represents the transcription factor family, and the *y*-axis represents the number of transcription factor genes.

3.6. JIP-Test Demonstrated Senescence Inhibited Leaf Photosynthetic Capacity

A standard OJIP analysis of the fluorescence induction curves and difference curve calculations were carried out to investigate the influence of senescence on photosynthesis. Induction curves revealed significantly lower fluorescence in senescent leaves (Figure S1A). The main difference between mature and senescent leaves was that senescent leaves had significantly higher levels of the relative variable fluorescence and high values for J level than mature leaves (Figures S1B and 3A). In the ΔVt curve of the senescent leaves compared to the mature leaves, we found a significant positive L-band and K-band (Figure 3B,C). In contrast, a negative H-band and G-band in senescent leaves were identified (Figure 3D,E).

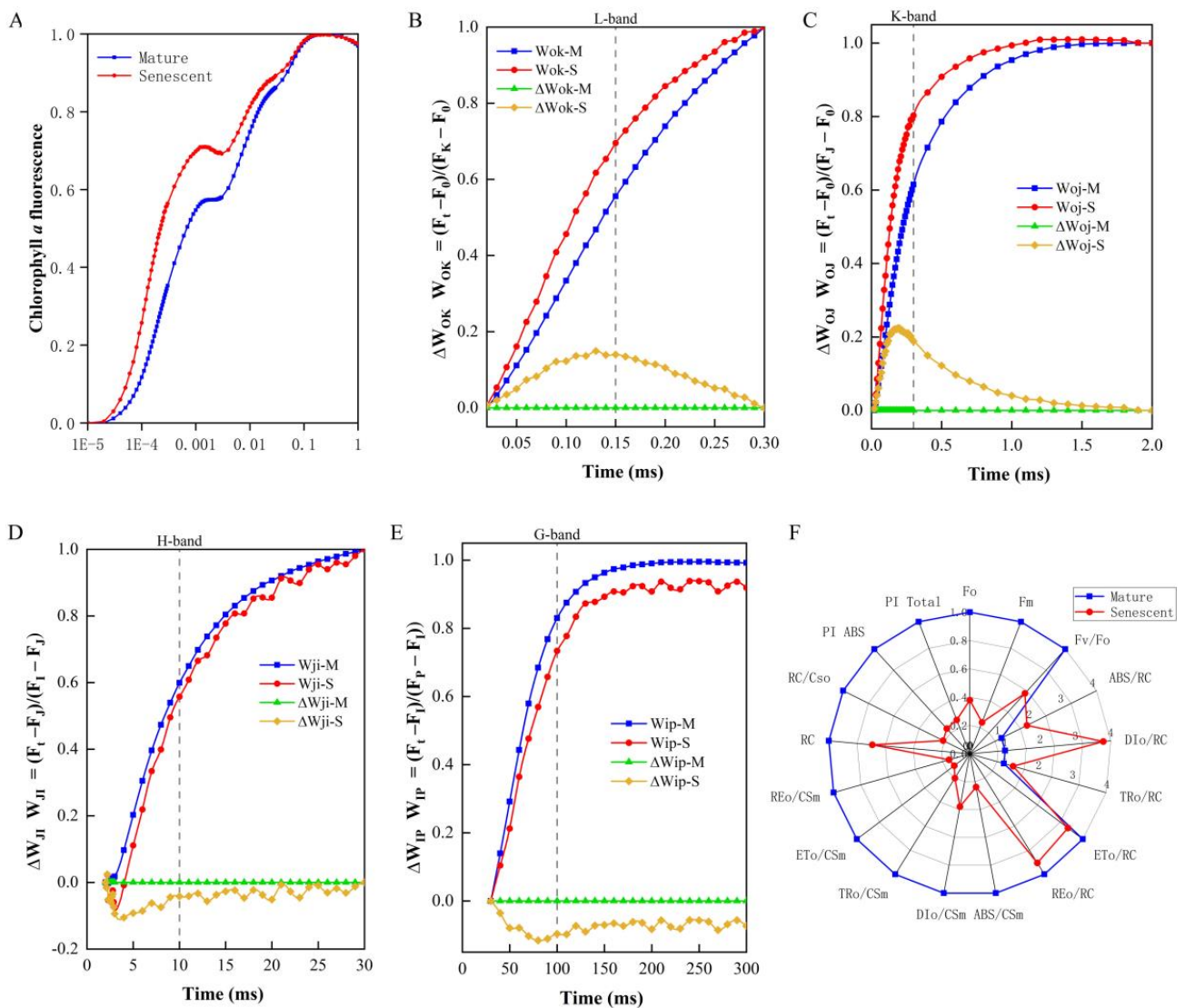


Figure 3. Chlorophyll fluorescence induction curves analysis in mature and senescent leaves. (A) The standard OJIP curves. (B) L-band. (C) K-band. (D) H-band. (E) G-band. (F) Radar plot of the fluorescence parameters. The fluorescence parameters were displayed as the means of 11 replicates. Four bands and the fluorescence parameters between mature and senescent leaves were significantly different at $p \leq 0.05$ based on Student’s *t*-test.

We acquired information about the structure and function of the primary PSII from the JIP-test parameters (Figure 3F). The definition of OJIP test parameters used in this study is shown in Table S9. There were lower values of F_o , F_m , and F_v/F_o in senescent leaves than in mature leaves due to a lower density of photosynthetic structures (RC/CSo).

The lower number of PSII reaction centers (RC) was significantly low in the senescent leaves ($p < 0.05$) (Figure 3F). In senescent leaves, we found higher values of ABS/RC and TRo/RC. However, the value of the parameter DIO/RC was 3.8 times that of mature leaves. Meanwhile, we found lower values of ETo/RC and REo/RC in senescent leaves. Much absorption and trapping excitation energy in senescent leaves was dissipated as heat in PSII antennae and reaction centers (Figures 3F and S1C). The density of active PSII reaction centers per cross-section (RC/CS_o) is five times lower in senescent leaves than in mature leaves, which affected the PSII efficiency in senescent leaves. The decreased PI_{ABS} and PI_{Total} indicated disturbed PSII, PSI, and the intersystem electron transport chain in senescent leaves. Furthermore, the reduced ABS/CS_m demonstrated the retarded energy absorption by PSII antenna pigments of senescent leaves. The declined TRo/CS_m revealed the reduced active reaction center and trapping energy fluxes. The decrease in ETo/CS_m presented passive electron transport. Furthermore, the dropped REo/CS_m suggested repressed the efficiency of PSI (Figures 3F and S1C).

3.7. Genes Regulating Chlorophyll Biosynthesis and Metabolism Are Involved in Leaf Senescence

Chloroplast development and degeneration play an essential role in plant leaf senescence. We identified DEGs regulating chloroplast biosynthesis and metabolism based on KEGG pathway annotations. This study identified 12 DEGs associated with chlorophyll biosynthesis and eight DEGs related to chlorophyll degradation. The expression profiles of genes encoding enzymes involved in these pathways were identified (Figure 4). A total of 12 chlorophyll biosynthesis genes were significantly downregulated in the senescent leaves, suggesting low chlorophyll biosynthesis efficiency. Moreover, the expression of three chlorophyll degradation-related genes (*NYC1* and two *RCCR* genes) was increased significantly in senescent leaves. The finding revealed that chlorophyll degradation genes were expressed substantially higher in the senescent leaves than in mature leaves.

Next, the DEGs involved in photosynthesis were analyzed. The genes encoding PsbO, PsbP, PabQ, PabR, PsbS, Pab27, and Psb28 proteins in PSII were repressed (Figure 5A). The suppressed expression of several PSI reaction center subunits genes in senescent leaves revealed the disaggregation of PSII and PSI. The retarded *PetC* encoding cytochrome *b6/f* complex subunits and the *alpha*, *delta*, and *b* subcomplexes of F-type ATPase indicated the declining efficiency of ATP synthesis. In addition, the suppressed *PetE*, *PetF*, *PetH*, and *PetJ* reflected intersystem electron transport between PSII and PSI. These results indicated that the DEGs involved in photosynthesis pathways play essential roles in leaf senescence. Moreover, DEGs in the light-harvesting chlorophyll protein complex (LHC), *Lhca1-6*, were all suppressed (Figure 5B).

3.8. Plant Hormone Responses during Leaf Senescence in *Z. japonica*

The pathway of plant hormone signal transduction (111 genes) was highly enriched and strongly linked with senescence. IAA, ET, and ABA pathways were identified, including their biosynthesis and related signal transduction. The expression profiles of genes encoding enzymes involved in these pathways were identified. During leaf senescence, 32 DEGs participated in IAA biosynthesis or signaling pathways (Figure 6). *TDC* and *TAA1* showed a coordinated down-regulation in IAA biosynthesis pathways, accompanied by changes in the expression of several IAA signaling genes. GH3 is mostly upregulated (3/4 shown), which is involved in auxin conjugation, consistent with reduced free IAA. However, the negative auxin signaling component (*TIR1*) is upregulated along with the auxin influx transporter (*AUX1*). *AUX/IAA* and *ARF* are large gene families with many functions related to auxin response, and some are upregulated while others are downregulated. Auxin may control senescence in part by activating gene expression. Furthermore, 22 DEGs mapped to the ABA biosynthesis and signal transduction pathways (Figure 7). The induction of *NCEDs* and *ABA2* activated the ABA biosynthesis pathway. The upregulated of *PYR/PYL*, *PP2C*, *SnRK2*, and *ABF* activated the ABA signal transduction pathway. In addition, 14 DEGs were mapped to ET biosynthesis and signal transduction pathways

(Figure 8). The result showed that the expression of *ACO* activated the ET biosynthesis pathway. The ET signal transduction pathway was upregulated by several genes (*CTR1*, *SIMKK*, and *EIN3*). In total, these results indicated that IAA biosynthesis was inhibited, ABA and ET biosynthesis were activated, and signal transduction for IAA, ABA, and ET were all activated.

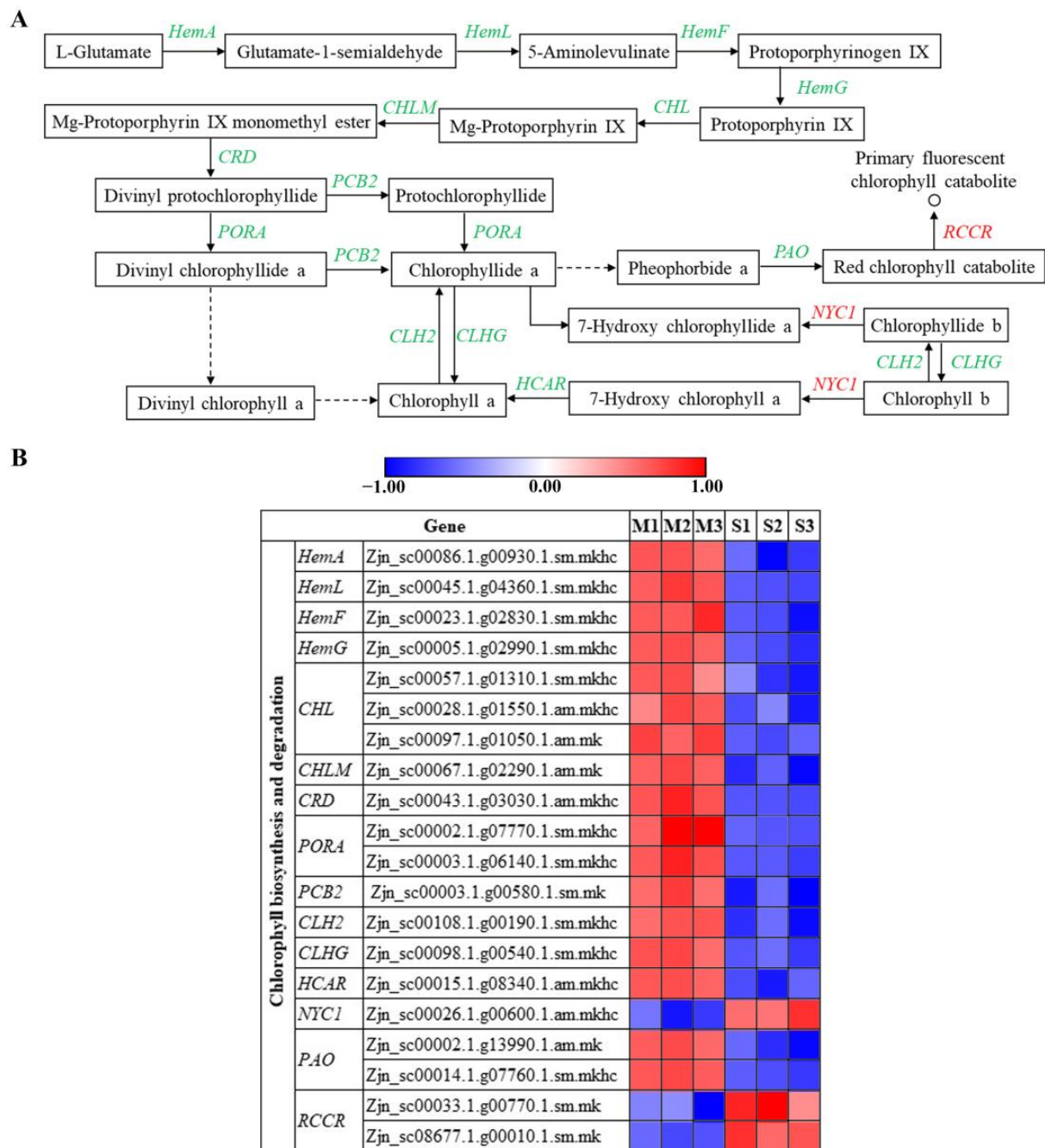


Figure 4. Expression profiles of DEGs involved in chlorophyll biosynthesis and degradation between mature and senescent leaves. (A) chlorophyll biosynthesis and degradation in *Z. japonica*. (B) Expression of genes involved in chlorophyll biosynthesis and degradation in *Z. japonica*. Plain text denotes substrates and products; italic denotes genes encoding enzymes. In the pathway, red represents upregulated genes; green represents downregulated genes.

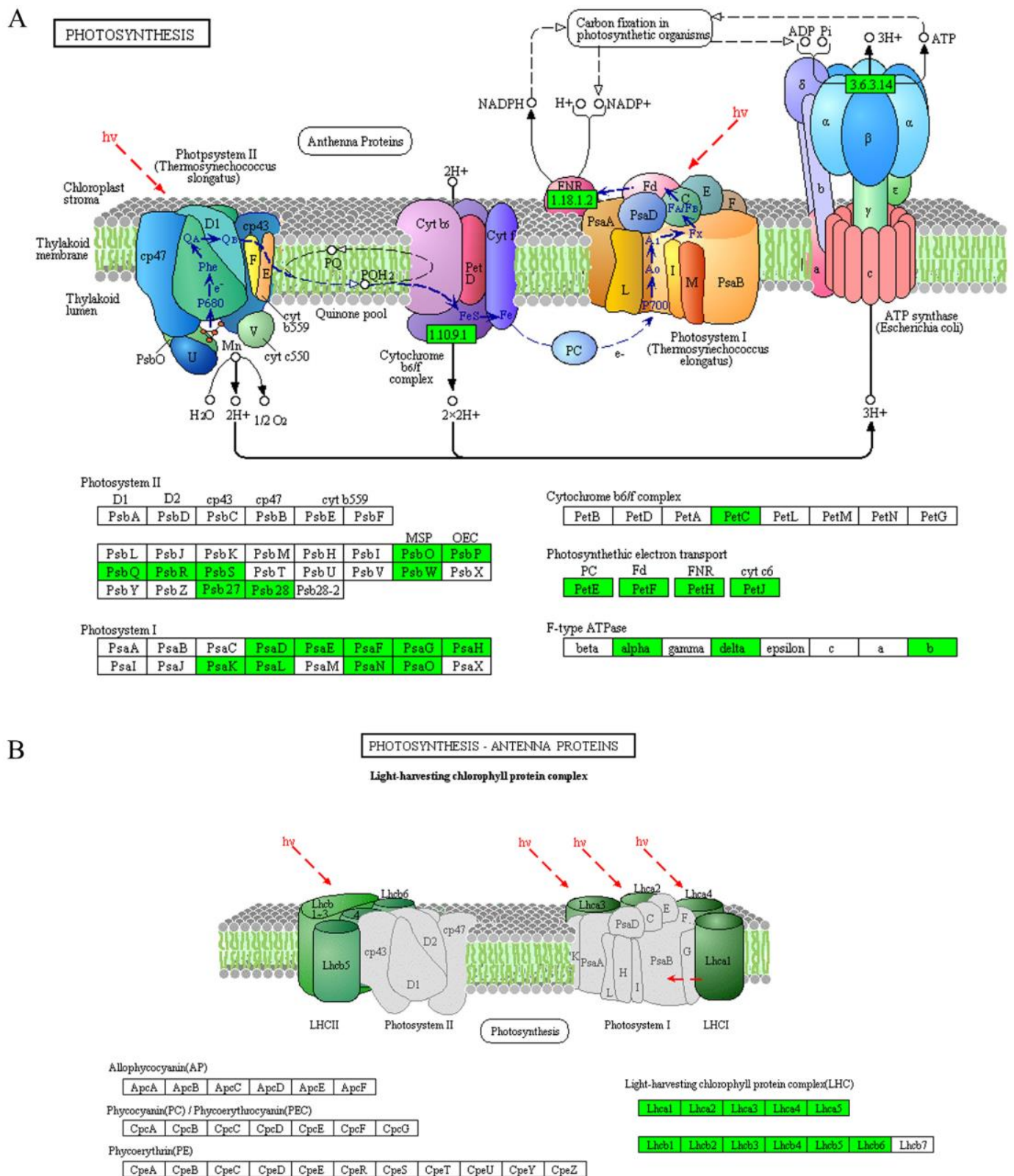


Figure 5. DEGs mapped to photosynthesis (A) and photosynthesis-antenna proteins (B) pathway between mature and senescent leaves in *Z. japonica*.

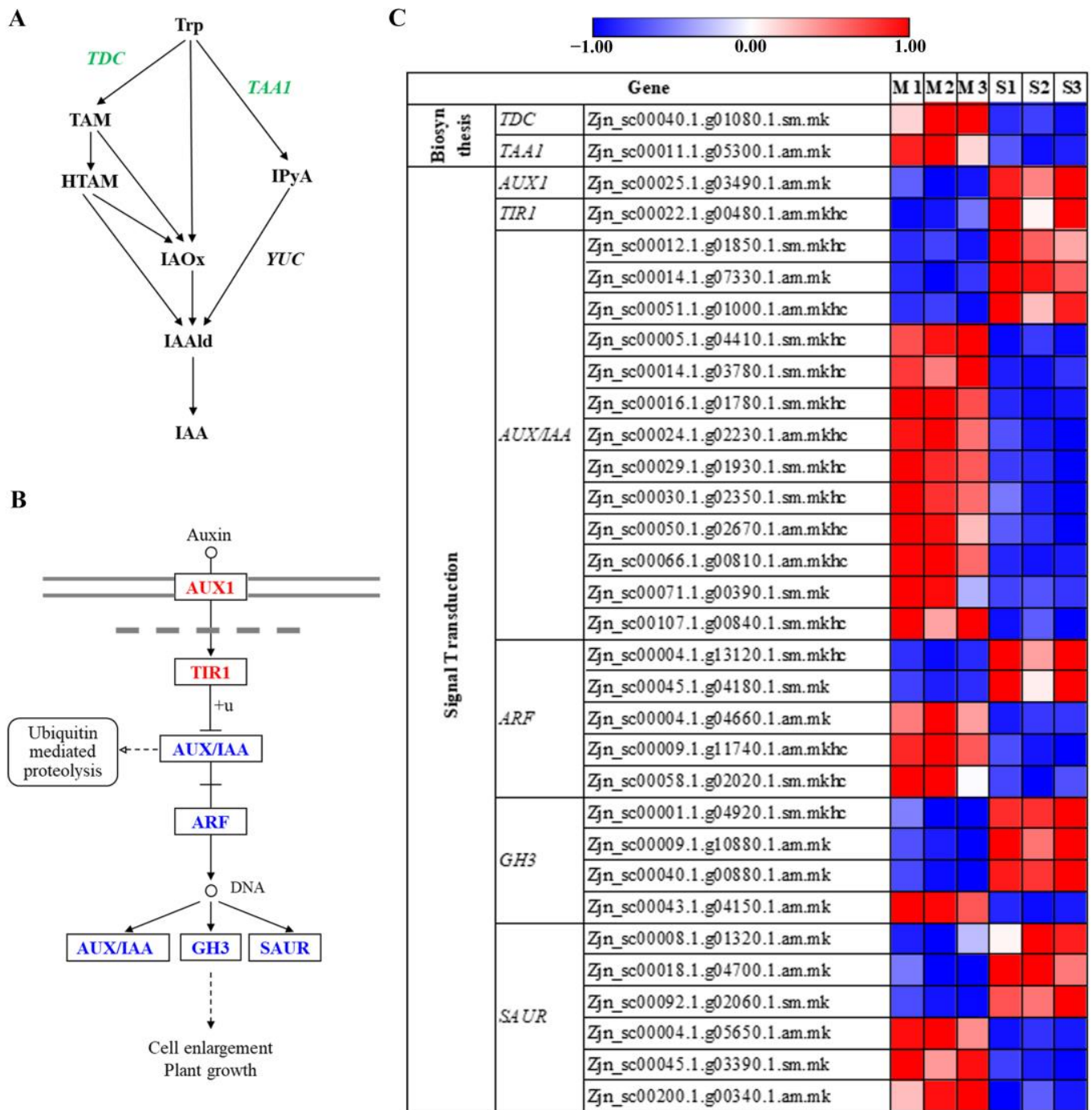


Figure 6. Expression profiles of DEGs involved in IAA biosynthesis and signal transduction genes between mature and senescent leaves. (A) IAA biosynthesis pathway in *Z. japonica*. (B) IAA signal transduction in *Z. japonica*. (C) Expression of genes involved in IAA biosynthesis and signal transduction. Plain text denotes substrates and products; italic denotes genes encoding enzymes. In the pathway, red represents upregulated genes, green represents downregulated genes, and blue represents upregulated and downregulated genes.

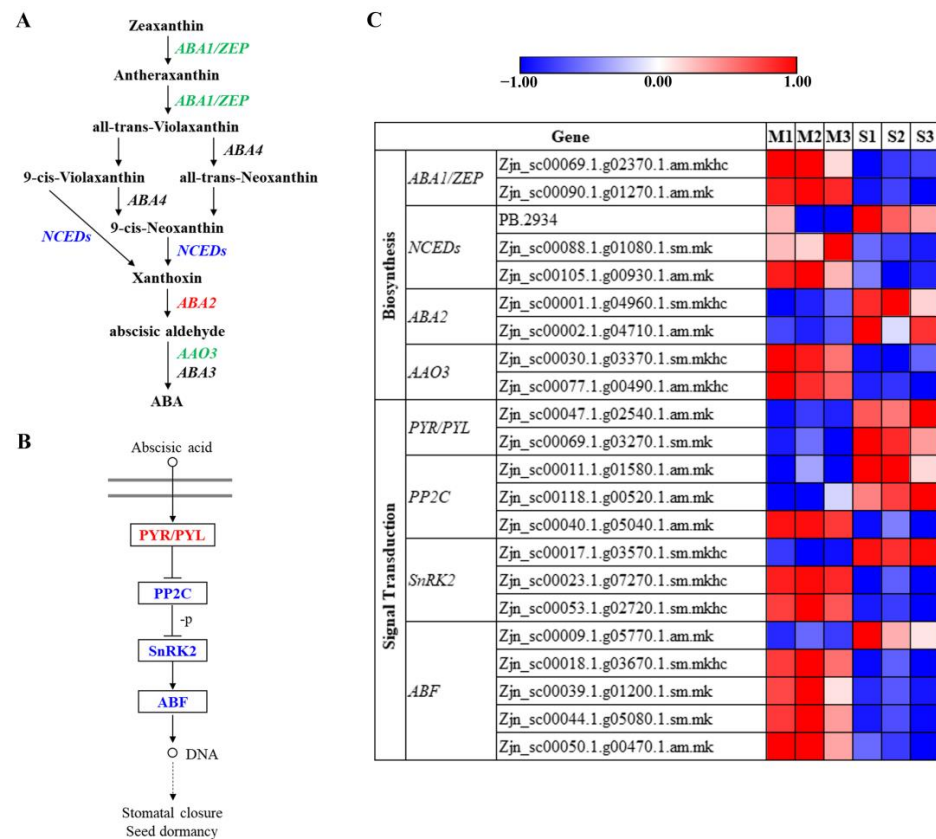


Figure 7. Expression profiles of DEGs involved in ABA biosynthesis and signal transduction genes between mature and senescent leaves. (A) ABA biosynthesis pathway in *Z. japonica*. (B) ABA signal transduction in *Z. japonica*. (C) Expression of genes involved in ABA biosynthesis and signal transduction. Plain text denotes substrates and products; italic denotes genes encoding enzymes. In the pathway, red represents upregulated genes, green represents downregulated genes, and blue represents upregulated and downregulated genes.

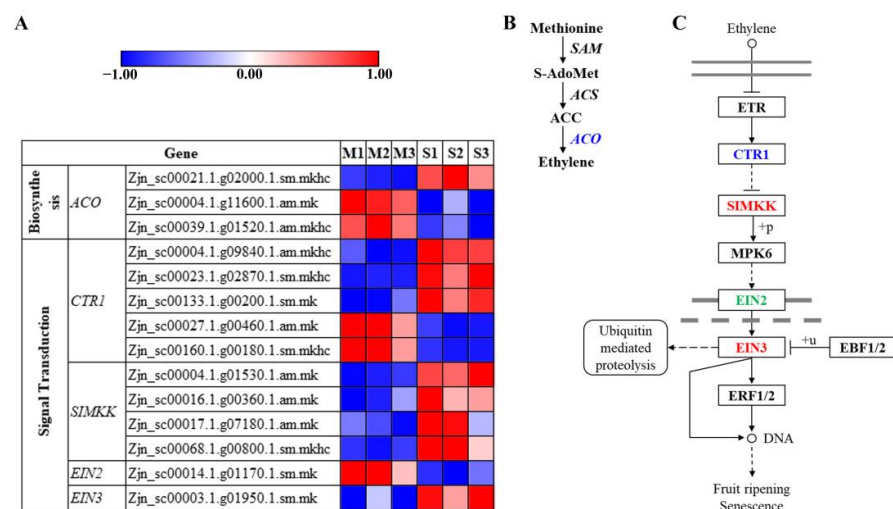


Figure 8. Expression profiles of DEGs involved in ET biosynthesis and signal transduction genes between mature and senescent leaves. (A) Expression of genes involved in ET biosynthesis and signal transduction. Plain text denotes substrates and products; italic denotes genes encoding enzymes. In the pathway, red represents upregulated genes, green represents downregulated genes, and blue represents upregulated and downregulated genes. (B) ET biosynthesis pathway in *Z. japonica*. (C) ET signal transduction in *Z. japonica*.

4. Discussion

Z. japonica is an important warm-season turfgrass with many excellent traits [45]. The genome sequence was published in 2016 [44]. The genome and full-length transcriptome data publications provide essential information resources for studying *Z. japonica* [45]. Previous Illumina RNA-seq studies on *Z. japonica* have mainly focused on mining the DEGs between different varieties [53] and exploring the molecular mechanism of salt adaptation [54,55]. Delayed leaf senescence is a crucial trait for the further utilization of *Z. japonica* in northern China. Nonetheless, the molecular mechanism involved in leaf senescence still needs to be well addressed. We present here the transcriptome and chlorophyll fluorescence test analysis of *Z. japonica* leaves during developmental senescence.

SAGs regulate the highly ordered leaf senescence process, and many SAGs were identified in various plants [6]. Recently, there were 3624 SAGs in cotton (*Gossypium hirsutum*), 3396 SAGs in sorghum (*Sorghum bicolor*), and 678 SAGs in poplar (*Populus trichocarpa*) identified [6,8,56]. The Leaf Senescence Database (LSD 4.0, May 2022; <https://ngdc.cnca.ac.cn/lsd>, accessed on 9 September 2022) documented 31,214 SAGs from 86 plant species. We compared all 4038 DEGs using the Leaf Senescence Database to analyze the sequence conservation between *Z. japonica* and other species. The result showed that 2515 DEGs have homologous genes. These matched known-function SAGs are mainly involved in chlorophyll degradation, plant hormone response, and lipid metabolism. This result is consistent with the reports of cotton, sorghum, and red clover (*Trifolium pratense*) [4,8,56]. Notably, 37.7% of the DEGs were not highly homologous to known SAGs, which indicated they might be unique to *Z. japonica* during leaf senescence. These results revealed a divergence in leaf senescence mechanisms between *Z. japonica* and other plants. The transcriptome information on *Z. japonica* could be beneficial for us to conduct a comparative analysis between herbaceous and woody plants.

A total of 539 differentially expressed TFs from 117 TF families were predicted, and 397 were also displayed in the SAGs analysis. TFs in the AP2/ERF-ERF, NAC, WRKY, bHLH, MYB, and bZIP families significantly overlap with senescence-associated TFs in *Arabidopsis* [7], suggesting that TF regulation of plant leaf senescence may be relatively conserved. AP2/ERF-ERF, the top TF family in leaf senescence of *Z. japonica*, includes 21 downregulated and 13 upregulated members. AP2/ERF-ERF genes were reported to participate in the transcriptional regulation of senescence processes [57]. Expression of an AP2/ERF-ERF transcription factor gene, *AtCBF2*, delays leaf senescence and extends plant longevity [58]. The NAC family plays a crucial role in modulating plant senescence. Expression of a NAC transcription factor gene, *BeNAC1*, resulted in various senescence phenotypes in *Arabidopsis* [59]. The NAC factor *LpNAL* delays leaf senescence by repressing two chlorophyll catabolic genes (*LpSGR* and *LpNYC1*) in perennial ryegrass [12]. There were 33 NAC genes, including 27 upregulated and six downregulated, in leaf senescence in *Z. japonica*. WRKY transcription factors, which play a central role in leaf senescence in *Arabidopsis* [23], are essential in *Z. japonica* equally.

Leaf color is an essential commercial trait for ornamental plants and turfgrasses [5]. The visible symptom of leaf senescence is yellowing, which results from preferential degradation of the green pigment chlorophyll [60]. With the breakdown of chloroplast and the loss of chlorophylls, the photosynthetic capacity of a leaf decreases sharply during senescence [60]. In this study, the chlorophyll content was decreased in senescent leaves. The findings were consistent with previous reports on *Z. japonica* and other plants [1,10,61]. In this study, all DEGs in the chlorophyll biosynthesis pathway were downregulated. *ZjNYC1*, a chlorophyll degradation-related gene, was significantly upregulated in senescent leaves, consistent with a previous report [10]. During the leaf senescence of *Z. japonica*, the contents of Chl, Chl *a*, and Chl *b* were all significantly reduced ($p < 0.01$). The above results showed that senescence represses chlorophyll biosynthesis, upregulating chlorophyll degradation. Moreover, the ratio of Chl *a*/Chl *b* is an effective indicator of leaf senescence [62,63]. In this study, the Chl *a*/Chl *b* levels in senescent leaves were decreased, consistent with previous reports in *Arabidopsis* and *Trifolium pratense* [4,63].

The course of Chl *a* fluorescence transitions during its characteristic phases O–K, O–J, J–I, and I–P help us understand the physiological state of the photosynthesizing object [64–67]. High values for the J level in the senescent leaves indicated lower (or even blocked) electron flow in the acceptor side of PSII [68]. The positive L-band is a sign of the ungrouping of the antenna pigment complex, and the positive K-band is a sign of the inactivation of the oxygen-evolving complex (OEC) [11,47]. It was in line with the downregulated expression of the genes, including *PsbO*, *PsbP*, *PabQ*, *PabR*, *PsbS*, *Pab27*, and *Psb28* in PSII [10]. The negative H-band represents the inhibited electron flow between PSII and PSI [10,68]. The suppression of genes encoding Cyt *b6/f*, which functions in the electron flow between PSII and PSI reaction centers, aided it [69]. The negative G-band revealed that the acceptor pool of PSI terminal electron acceptor is relatively large, whereas the transcriptional level of genes in PSI was downregulated. The results indicated the inhibition of PSI activity. The significantly lower RE_o/CS_m levels were consistent with the results. JIP-test parameters better visualize the differences between mature and senescent leaves in *Z. japonica* [65]. The lower F_o, F_m, and F_v/F_o mean less photosynthetic material in senescent leaves [68]. We compared the parameters per PSII reaction center, and the energy transfer in mature leaves is much more effective than in senescent leaves. The JIP-test analysis showed that senescence negatively affects the integrity and functionality of PSII, PSI, and the intersystem electron transport chain. It corresponded to the reduced transcriptional level of genes encoding photosynthetic electron transport, F-type ATPase, and LHC protein complexes.

Various phytohormones can induce or suppress leaf senescence [25]. Previous studies showed that changes in IAA signaling and transport could be significant in modulating the senescence of *Gossypium hirsutum* [8]. However, although a suppressing effect of IAA on senescence was previously reported [70], the function of IAA in senescence is poorly understood. In *Z. japonica*, IAA content decreased, the IAA biosynthesis pathway was inhibited, and the IAA signal transduction pathway was activated. Therefore, we predicted that endogenous IAA levels and signal transduction play crucial roles in modulating leaf senescence in *Z. japonica*.

ABA is considered an enhancer rather than a triggering factor of leaf senescence [3,70]. During leaf senescence in *Z. japonica*, changes in the expression of several ABA biosynthesis components occur. The ABA receptor PYR/PYL family proteins were significantly upregulated, demonstrating that the ABA signaling pathway is active during leaf senescence in *Z. japonica*. Moreover, ABA content increased with the progression of leaf senescence. It corresponded to the previous report on *Arabidopsis* [8,70]. ET has been considered a critical hormone in regulating leaf senescence [3,70]. The ET biosynthesis and signal transduction were activated with the induction of *ACO*, *CTR1*, *SIMKK*, and *EIN3*. It corresponded to the previous report [10,70].

5. Conclusions

In conclusion, an integrated analysis of RNA-seq and JIP-test was used to analyze the senescence processes in *Z. japonica*. A total of 4038 DEGs, 2515 candidate SAGs, and 539 TFs were identified in leaf senescence. Furthermore, the IAA biosynthesis was inhibited, ET and ABA biosynthesis were activated, and signal transduction of IAA, ET, and ABA were all activated in leaf senescence. In addition, senescence represses chlorophyll biosynthesis, upregulates chlorophyll degradation, and negatively affects the integrity and functionality of PSII, PSI, and the intersystem electron transport chain. These results add to our understanding of the regulatory mechanism of leaf senescence. The senescence-associated genes are candidate targets to provide new insight for leaf senescence modeling in *Z. japonica*. They provided a theoretical foundation to reveal the functions of senescence-associated genes and chlorophyll catabolic genes involved in leaf senescence.

Supplementary Materials: The following supporting information can be downloaded at: <https://www.mdpi.com/article/10.3390/agronomy13030623/s1>, Figure S1: Chlorophyll fluorescence induction curves analysis in mature and senescent leaves. (A) The OJIP curves. (B) The relative variable fluorescence V_t of the transient chlorophyll a fluorescence. (C) The proportion of phenomenological energy flux parameters in mature and senescent leaves displayed by the leaf pipeline model. The fluorescence parameters were displayed as means of 11 replicates. The width of the arrow represents the relative values of the associated parameters; dark circle represents non-active reaction centers; Table S1: All genes identified by RNA-seq at mature and senescent stages in *Z. japonica*; Table S2: List of genes that are differentially expressed during leaf senescence processes in *Z. japonica*; Table S3: List of primers used for q RT-PCR; Table S4: List of leaf senescence orthologs between *Z. japonica* and other species; Table S5: Enriched GO terms in biological process, cellular component, and molecular function; Table S6: Enriched upregulated pathways identified by KOBAS during leaf senescence in *Z. japonica*; Table S7: Enriched downregulated pathways identified by KOBAS during leaf senescence in *Z. japonica*; Table S8: List of transcription factor DEGs during leaf senescence in *Z. japonica*; Table S9: Summary of the OJIP test parameters used in this study.

Author Contributions: Conceptualization, K.T. and S.Y.; data curation, J.G., X.F. and Y.Y.; formal analysis, J.G. and S.Y.; funding acquisition, K.T.; investigation, J.G.; methodology, L.X.; project administration, J.G., X.F. and Y.Y.; resources, K.T.; software, L.X.; supervision, K.T.; validation, J.G.; visualization, J.G.; writing—original draft, J.G.; writing—review and editing, K.T. and S.Y. All authors have read and agreed to the published version of the manuscript.

Funding: This study was supported by the National Natural Science Foundation of China (No.31901397) and the Scientific Funds of Beijing Academy of Agriculture and Forestry Sciences (KJ CX20210431, KJ CX20220103).

Institutional Review Board Statement: Not applicable.

Informed Consent Statement: Not applicable.

Data Availability Statement: The Illumina NGS reads generated in this study were submitted to the BioProject database of the National Center for Biotechnology Information (accession numbers PRJNA775807).

Acknowledgments: We acknowledge the Biomarker Corporation (Beijing, China) for the facilities and expertise of the Illumina platform for library construction and sequencing. The authors would like to thank Kai Wang from Hansha Scientific Instruments Ltd. for the Handy PEA parameter analysis.

Conflicts of Interest: The authors declare that they have no competing interest.

References

- Lim, P.O.; Kim, H.J.; Nam, H.G. Leaf Senescence. *Annu. Rev. Plant Biol.* **2007**, *58*, 115–136. [[CrossRef](#)]
- Gao, S.; Gao, J.; Zhu, X.; Song, Y.; Li, Z.; Ren, G.; Zhou, X.; Kuai, B. ABF2, ABF3, and ABF4 promote ABA-mediated chlorophyll degradation and leaf senescence by transcriptional activation of chlorophyll catabolic genes and senescence-associated genes in *Arabidopsis*. *Mol. Plant* **2016**, *9*, 1272–1285. [[CrossRef](#)]
- Schippers, J.H.M.; Schmidt, R.; Wagstaff, C.; Jing, H.-C. Living to die and dying to live: The survival strategy behind leaf senescence. *Plant Physiol.* **2015**, *169*, 914–930. [[CrossRef](#)]
- Chao, Y.; Xie, L.; Yuan, J.; Guo, T.; Li, Y.; Liu, F.; Han, L. Transcriptome analysis of leaf senescence in red clover (*Trifolium pratense* L.). *Physiol. Mol. Biol. Plants* **2018**, *24*, 753–765. [[CrossRef](#)]
- Xu, B.; Li, H.; Li, Y.; Yu, G.; Zhang, J.; Huang, B. Characterization and transcriptional regulation of chlorophyll *b* reductase gene *NON-YELLOW COLORING 1* associated with leaf senescence in perennial ryegrass (*Lolium perenne* L.). *Environ. Exp. Bot.* **2018**, *149*, 43–50. [[CrossRef](#)]
- Li, Z.; Zhang, Y.; Zou, D.; Zhao, Y.; Wang, H.-L.; Zhang, Y.; Xia, X.; Luo, J.; Guo, H.; Zhang, Z. LSD 3.0: A comprehensive resource for the leaf senescence research community. *Nucleic Acids Res.* **2020**, *48*, D1069–D1075. [[CrossRef](#)]
- Kim, J.; Woo, H.R.; Nam, H.G. Toward systems understanding of leaf senescence: An integrated multi-omics perspective on leaf senescence research. *Mol. Plant* **2016**, *9*, 813–825. [[CrossRef](#)]
- Lin, M.; Pang, C.; Fan, S.; Song, M.; Wei, H.; Yu, S. Global analysis of the *Gossypium hirsutum* L. Transcriptome during leaf senescence by RNA-Seq. *BMC Plant Biol.* **2015**, *15*, 43. [[CrossRef](#)]
- Zhang, J.; Yu, G.; Wen, W.; Ma, X.; Xu, B.; Huang, B. Functional characterization and hormonal regulation of the *PHEOPHYTINASE* gene *LpPPH* controlling leaf senescence in perennial ryegrass. *J. Exp. Bot.* **2016**, *67*, 935–945. [[CrossRef](#)]

10. Teng, K.; Tan, P.; Guan, J.; Dong, D.; Liu, L.; Guo, Y.; Guo, W.; Yuesen, Y.; Fan, X.; Wu, J. Functional characterization of the chlorophyll b reductase gene *NYC1* associated with chlorophyll degradation and photosynthesis in *Zoysia japonica*. *Environ. Exp. Bot.* **2021**, *191*, 104607. [[CrossRef](#)]
11. Teng, K.; Han, C.; Yue, Y.; Xu, L.; Li, H.; Wu, J.; Fan, X. Functional characterization of the pheophytinase gene, *ZjPPH*, from *Zoysia japonica* in regulating chlorophyll degradation and photosynthesis. *Front. Plant Sci.* **2021**, *12*, 786570. [[CrossRef](#)]
12. Yu, G.; Xie, Z.; Lei, S.; Li, H.; Xu, B.; Huang, B. The NAC factor LpNAL delays leaf senescence by repressing two chlorophyll catabolic genes in perennial ryegrass. *Plant Physiol.* **2022**, *189*, 595–610. [[CrossRef](#)]
13. Balazadeh, S.; Riaño-Pachón, D.; Mueller-Roeber, B. Transcription factors regulating leaf senescence in *Arabidopsis thaliana*. *Plant Biol.* **2008**, *10*, 63–75. [[CrossRef](#)]
14. Xu, H.; Wang, X.; Chen, J. Overexpression of the *Rap2.4f* transcriptional factor in *Arabidopsis* promotes leaf senescence. *Sci. China Life Sci.* **2010**, *53*, 1221–1226. [[CrossRef](#)]
15. Yang, S.-D.; Seo, P.J.; Yoon, H.-K.; Park, C.-M. The *Arabidopsis* NAC Transcription Factor VNI2 Integrates Abscisic Acid Signals into Leaf Senescence via the *COR/RD* Genes. *Plant Cell* **2011**, *23*, 2155–2168. [[CrossRef](#)]
16. Farage-Barhom, S.; Burd, S.; Sonego, L.; Mett, A.; Belausov, E.; Gidoni, D.; Lers, A. Localization of the *Arabidopsis* senescence- and cell death-associated BFN1 nuclease: From the ER to fragmented nuclei. *Mol. Plant* **2011**, *4*, 1062–1073. [[CrossRef](#)]
17. Matallana-Ramirez, L.P.; Rauf, M.; Farage-Barhom, S.; Dortay, H.; Xue, G.-P.; Dröge-Laser, W.; Lers, A.; Balazadeh, S.; Mueller-Roeber, B. NAC transcription factor ORE1 and senescence-induced *BIFUNCTIONAL NUCLEASE1 (BFN1)* constitute a regulatory cascade in *Arabidopsis*. *Mol. Plant* **2013**, *6*, 1438–1452. [[CrossRef](#)]
18. Qiu, K.; Li, Z.; Yang, Z.; Chen, J.; Wu, S.; Zhu, X.; Gao, S.; Gao, J.; Ren, G.; Kuai, B.; et al. EIN3 and ORE1 Accelerate Degreening during Ethylene-Mediated Leaf Senescence by Directly Activating Chlorophyll Catabolic Genes in *Arabidopsis*. *PLoS Genet.* **2015**, *11*, e1005399. [[CrossRef](#)]
19. Guo, Y.; Gan, S. AtNAP, a NAC family transcription factor, has an important role in leaf senescence. *Plant J.* **2006**, *46*, 601–612. [[CrossRef](#)]
20. Zhang, K.; Gan, S.-S. An abscisic acid-AtNAP transcription factor-SAG113 protein phosphatase 2C regulatory chain for controlling dehydration in senescing *Arabidopsis* leaves. *Plant Physiol.* **2012**, *158*, 961–969. [[CrossRef](#)]
21. Rinerson, C.I.; Scully, E.D.; Palmer, N.A.; Donze-Reiner, T.; Rabara, R.C.; Tripathi, P.; Shen, Q.J.; Sattler, S.E.; Rohila, J.S.; Sarath, G.; et al. The WRKY transcription factor family and senescence in switchgrass. *BMC Genom.* **2015**, *16*, 912. [[CrossRef](#)]
22. Jaradat, M.R.; Feurtado, J.A.; Huang, D.; Lu, Y.; Cutler, A.J. Multiple roles of the transcription factor AtMYBR1/AtMYB44 in ABA signaling, stress responses, and leaf senescence. *BMC Plant Biol.* **2013**, *13*, 192. [[CrossRef](#)]
23. Miao, Y.; Zentgraf, U. A HECT E3 ubiquitin ligase negatively regulates *Arabidopsis* leaf senescence through degradation of the transcription factor WRKY53. *Plant J.* **2010**, *63*, 179–188. [[CrossRef](#)]
24. Besseau, S.; Li, J.; Palva, E.T. WRKY54 and WRKY70 co-operate as negative regulators of leaf senescence in *Arabidopsis thaliana*. *J. Exp. Bot.* **2012**, *63*, 2667–2679. [[CrossRef](#)]
25. Li, Z.; Peng, J.; Wen, X.; Guo, H. Gene Network Analysis and Functional Studies of Senescence-associated Genes Reveal Novel Regulators of *Arabidopsis* Leaf Senescence. *J. Integr. Plant Biol.* **2012**, *54*, 526–539. [[CrossRef](#)]
26. Bajguz, A.; Piotrowska, A. Conjugates of auxin and cytokinin. *Phytochemistry* **2009**, *70*, 957–969. [[CrossRef](#)]
27. Chen, Q.; Westfall, C.S.; Hicks, L.M.; Wang, S.; Jez, J.M. Kinetic basis for the conjugation of auxin by a GH3 family indole-acetic acid-amido synthetase. *J. Biol. Chem.* **2010**, *285*, 29780–29786. [[CrossRef](#)]
28. Kim, J.I.; Murphy, A.S.; Baek, D.; Lee, S.-W.; Yun, D.-J.; Bressan, R.A.; Narasimhan, M.L. *YUCCA6* over-expression demonstrates auxin function in delaying leaf senescence in *Arabidopsis thaliana*. *J. Exp. Bot.* **2011**, *62*, 3981–3992. [[CrossRef](#)]
29. Urano, K.; Maruyama, K.; Jikumaru, Y.; Kamiya, Y.; Yamaguchi-Shinozaki, K.; Shinozaki, K. Analysis of plant hormone profiles in response to moderate dehydration stress. *Plant J.* **2017**, *90*, 17–36. [[CrossRef](#)]
30. Kieber, J.J.; Schaller, G.E. Cytokinins. *Arab. Book/Am. Soc. Plant Biol.* **2014**, *12*, e0168. [[CrossRef](#)]
31. Wasternack, C.; Hause, B. Jasmonates: Biosynthesis, perception, signal transduction and action in plant stress response, growth and development. An update to the 2007 review in *Annals of Botany*. *Ann. Bot.* **2013**, *111*, 1021–1058. [[CrossRef](#)]
32. Yu, X.; Xu, Y.; Yan, S. Salicylic acid and ethylene coordinately promote leaf senescence. *J. Integr. Plant Biol.* **2021**, *63*, 823–827. [[CrossRef](#)]
33. Wang, C.; Dai, S.; Zhang, Z.L.; Lao, W.; Wang, R.; Meng, X.; Zhou, X. Ethylene and salicylic acid synergistically accelerate leaf senescence in *Arabidopsis*. *J. Integr. Plant Biol.* **2021**, *63*, 828–833. [[CrossRef](#)]
34. Kim, H.J.; Hong, S.H.; Kim, Y.W.; Lee, I.H.; Jun, J.H.; Phee, B.-K.; Rupak, T.; Jeong, H.; Lee, Y.; Hong, B.S. Gene regulatory cascade of senescence-associated NAC transcription factors activated by ETHYLENE-INSENSITIVE2-mediated leaf senescence signalling in *Arabidopsis*. *J. Exp. Bot.* **2014**, *65*, 4023–4036. [[CrossRef](#)]
35. Kim, J.H.; Woo, H.R.; Kim, J.; Lim, P.O.; Lee, I.C.; Choi, S.H.; Hwang, D.; Nam, H.G. Trifurcate feed-forward regulation of age-dependent cell death involving *miR164* in *Arabidopsis*. *Science* **2009**, *323*, 1053–1057. [[CrossRef](#)]
36. Li, Z.; Peng, J.; Wen, X.; Guo, H. *Ethylene-insensitive3* is a senescence-associated gene that accelerates age-dependent leaf senescence by directly repressing *miR164* transcription in *Arabidopsis*. *Plant Cell* **2013**, *25*, 3311–3328. [[CrossRef](#)]
37. Zhao, Y.; Chan, Z.; Gao, J.; Xing, L.; Cao, M.; Yu, C.; Hu, Y.; You, J.; Shi, H.; Zhu, Y. ABA receptor PYL9 promotes drought resistance and leaf senescence. *Proc. Natl. Acad. Sci. USA* **2016**, *113*, 1949–1954. [[CrossRef](#)]

38. Patton, A.J.; Reicher, Z.J. Zoysiagrass species and genotypes differ in their winter injury and freeze tolerance. *Crop Sci.* **2007**, *47*, 1619–1627. [[CrossRef](#)]
39. Kimball, J.A.; Zuleta, M.C.; Kenworthy, K.E.; Lehman, V.G.; Harris-Shultz, K.R.; Milla-Lewis, S. Genetic relationships in *Zoysia* species and the identification of putative interspecific hybrids using simple sequence repeat markers and inflorescence traits. *Crop Sci.* **2013**, *53*, 285–295. [[CrossRef](#)]
40. Tanaka, H.; Tokunaga, R.; Muguerza, M.; Kitazaki, Y.; Hashiguchi, M.; Sato, S.; Tabata, S.; Akashi, R. Genetic structure and speciation of zoysiagrass ecotypes collected in Japan. *Crop Sci.* **2016**, *56*, 818–826. [[CrossRef](#)]
41. Teng, K.; Tan, P.; Xiao, G.; Han, L.; Chang, Z.; Chao, Y. Heterologous expression of a novel *Zoysia japonica* salt-induced glycine-rich RNA-binding protein gene, *ZjGRP*, caused salt sensitivity in *Arabidopsis*. *Plant Cell Rep.* **2017**, *36*, 179–191. [[CrossRef](#)]
42. Teng, K.; Tan, P.; Guo, W.; Yue, Y.; Fan, X.; Wu, J. Heterologous expression of a novel *Zoysia japonica* C₂H₂ zinc finger gene, *ZjZFN1*, improved salt tolerance in *Arabidopsis*. *Front. Plant Sci.* **2018**, *9*, 1159. [[CrossRef](#)]
43. Teng, K.; Chang, Z.; Li, X.; Sun, X.; Liang, X.; Xu, L.; Chao, Y.; Han, L. Functional and RNA-sequencing analysis revealed expression of a novel stay-green gene from *Zoysia japonica* (*ZjSGR*) caused chlorophyll degradation and accelerated senescence in *Arabidopsis*. *Front. Plant Sci.* **2016**, *7*, 1894. [[CrossRef](#)]
44. Tanaka, H.; Hirakawa, H.; Kosugi, S.; Nakayama, S.; Ono, A.; Watanabe, A.; Hashiguchi, M.; Gondo, T.; Ishigaki, G.; Muguerza, M.; et al. Sequencing and comparative analyses of the genomes of zoysiagrasses. *DNA Res.* **2016**, *23*, 171–180. [[CrossRef](#)]
45. Guan, J.; Yin, S.; Yue, Y.; Liu, L.; Guo, Y.; Zhang, H.; Fan, X.; Teng, K. Single-molecule long-read sequencing analysis improves genome annotation and sheds new light on the transcripts and splice isoforms of *Zoysia japonica*. *BMC Plant Biol.* **2022**, *22*, 263. [[CrossRef](#)]
46. Hoagland, D.R.; Arnon, D.I. The water-culture method for growing plants without soil. *Circ. Calif. Agric. Exp. Stn.* **1950**, *347*, 32.
47. Guan, J.; Teng, K.; Yue, Y.; Guo, Y.; Liu, L.; Yin, S.; Han, L. *Zoysia japonica* chlorophyll *b* reductase gene *NOL* participates in chlorophyll degradation and photosynthesis. *Front. Plant Sci.* **2022**, *13*, 906018. [[CrossRef](#)]
48. Kim, D.; Paggi, J.M.; Park, C.; Bennett, C.; Salzberg, S.L. Graph-based genome alignment and genotyping with HISAT2 and HISAT-genotype. *Nat. Biotechnol.* **2019**, *37*, 907–915. [[CrossRef](#)]
49. Trapnell, C.; Williams, B.A.; Pertea, G.; Mortazavi, A.; Kwan, G.; Van Baren, M.J.; Salzberg, S.L.; Wold, B.J.; Pachter, L. Transcript assembly and quantification by RNA-Seq reveals unannotated transcripts and isoform switching during cell differentiation. *Nat. Biotechnol.* **2010**, *28*, 511–515. [[CrossRef](#)]
50. Love, M.I.; Huber, W.; Anders, S. Moderated estimation of fold change and dispersion for RNA-seq data with DESeq2. *Genome Biol.* **2014**, *15*, 550. [[CrossRef](#)]
51. Young, M.D.; Wakefield, M.J.; Smyth, G.K.; Oshlack, A. Gene ontology analysis for RNA-seq: Accounting for selection bias. *Genome Biol.* **2010**, *11*, R14. [[CrossRef](#)]
52. Xie, C.; Mao, X.; Huang, J.; Ding, Y.; Wu, J.; Dong, S.; Kong, L.; Gao, G.; Li, C.-Y.; Wei, L. KOBAS 2.0: A web server for annotation and identification of enriched pathways and diseases. *Nucleic Acids Res.* **2011**, *39*, W316–W322. [[CrossRef](#)]
53. Ahn, J.H.; Kim, J.-S.; Kim, S.; Soh, H.Y.; Shin, H.; Jang, H.; Ryu, J.H.; Kim, A.; Yun, K.-Y.; Kim, S.; et al. *De Novo* Transcriptome Analysis to Identify Anthocyanin Biosynthesis Genes Responsible for Tissue-Specific Pigmentation in Zoysiagrass (*Zoysia japonica* Steud.). *PLoS ONE* **2015**, *10*, e0124497. [[CrossRef](#)]
54. Xie, Q.; Niu, J.; Xu, X.; Xu, L.; Zhang, Y.; Fan, B.; Liang, X.; Zhang, L.; Yin, S.; Han, L. *De novo* assembly of the Japanese lawngrass (*Zoysia japonica* Steud.) root transcriptome and identification of candidate unigenes related to early responses under salt stress. *Front. Plant Sci.* **2015**, *6*, 610.
55. Wang, J.; An, C.; Guo, H.; Yang, X.; Chen, J.; Zong, J.; Li, J.; Liu, J. Physiological and transcriptomic analyses reveal the mechanisms underlying the salt tolerance of *Zoysia japonica* Steud. *BMC Plant Biol.* **2020**, *20*, 114. [[CrossRef](#)]
56. Wu, X.-Y.; Hu, W.-J.; Luo, H.; Xia, Y.; Zhao, Y.; Wang, L.-D.; Zhang, L.-M.; Luo, J.-C.; Jing, H.-C. Transcriptome profiling of developmental leaf senescence in sorghum (*Sorghum bicolor*). *Plant Mol. Biol.* **2016**, *92*, 555–580. [[CrossRef](#)]
57. Liu, J.; Li, J.; Wang, H.; Fu, Z.; Liu, J.; Yu, Y. Identification and expression analysis of *ERF* transcription factor genes in petunia during flower senescence and in response to hormone treatments. *J. Exp. Bot.* **2011**, *62*, 825–840. [[CrossRef](#)]
58. Sharabi-Schwager, M.; Lers, A.; Samach, A.; Guy, C.L.; Porat, R. Overexpression of the *CBF2* transcriptional activator in *Arabidopsis* delays leaf senescence and extends plant longevity. *J. Exp. Bot.* **2010**, *61*, 261–273. [[CrossRef](#)]
59. Chen, Y.; Qiu, K.; Kuai, B.; Ding, Y. Identification of an NAP-like transcription factor *BeNAC1* regulating leaf senescence in bamboo (*Bambusa emeiensis* ‘Viridiflavus’). *Physiol. Plant.* **2011**, *142*, 361–371. [[CrossRef](#)]
60. Gan, S. The hormonal regulation of senescence. In *Plant Hormones: Biosynthesis, Signal Transduction, Action!* Davies, P.J., Ed.; Springer: Dordrecht, The Netherlands, 2010; pp. 597–617.
61. Hebbar, K.B.; Rane, J.; Ramana, S.; Panwar, N.R.; Ajay, S.; Rao, A.S.; Prasad, P.V.V. Natural variation in the regulation of leaf senescence and relation to N and root traits in wheat. *Plant Soil* **2014**, *378*, 99–112. [[CrossRef](#)]
62. Pruzinská, A.; Tanner, G.; Aubry, S.; Anders, I.; Moser, S.; Müller, T.; Ongania, K.-H.; Kräutler, B.; Youn, J.-Y.; Liljegren, S.J.; et al. Chlorophyll breakdown in senescent *Arabidopsis* leaves. characterization of chlorophyll catabolites and of chlorophyll catabolic enzymes involved in the degreening reaction. *Plant Physiol.* **2005**, *139*, 52–63. [[CrossRef](#)]
63. Schelbert, S.; Aubry, S.; Burla, B.; Agne, B.; Kessler, F.; Krupinska, K.; Hörtensteiner, S. Pheophytin pheophorbide hydrolase (pheophytinase) is involved in chlorophyll breakdown during leaf senescence in *Arabidopsis*. *Plant Cell* **2009**, *21*, 767–785. [[CrossRef](#)]

64. Baker, N.R. Chlorophyll fluorescence: A probe of photosynthesis in vivo. *Annu. Rev. Plant Biol.* **2008**, *59*, 89–113. [[CrossRef](#)]
65. Bussotti, F.; Desotgiu, R.; Pollastrini, M.; Cascio, C. The JIP test: A tool to screen the capacity of plant adaptation to climate change. *Scand. J. For. Res.* **2010**, *25*, 43–50. [[CrossRef](#)]
66. Kalaji, H.M.; Oukarroum, A.; Alexandrov, V.; Kouzmanova, M.; Brestic, M.; Zivcak, M.; Samborska, I.A.; Cetner, M.D.; Al-lakhverdiev, S.I.; Goltsev, V. Identification of nutrient deficiency in maize and tomato plants by in vivo chlorophyll *a* fluorescence measurements. *Plant Physiol. Biochem.* **2014**, *81*, 16–25. [[CrossRef](#)]
67. Sitko, K.; Rusinowski, S.; Kalaji, H.M.; Szopiński, M.; Małkowski, E. Photosynthetic efficiency as bioindicator of environmental pressure in *A. halleri*. *Plant Physiol.* **2017**, *175*, 290–302. [[CrossRef](#)]
68. Zagorchev, L.; Atanasova, A.; Albanova, I.; Traianova, A.; Mladenov, P.; Kouzmanova, M.; Goltsev, V.; Kalaji, H.M.; Teofanova, D. Functional characterization of the photosynthetic machinery in *Smicronix* galls on the parasitic plant *Cuscuta campestris* by JIP-Test. *Cells* **2021**, *10*, 1399. [[CrossRef](#)]
69. Eichelmann, H.; Price, D.; Badger, M.; Laisk, A. Photosynthetic parameters of leaves of wild type and Cyt *b₆/f* deficient transgenic Tobacco studied by CO₂ uptake and transmittance at 800 nm. *Plant Cell Physiol.* **2000**, *41*, 432–439. [[CrossRef](#)]
70. Zhang, H.; Zhou, C. Signal transduction in leaf senescence. *Plant Mol. Biol.* **2013**, *82*, 539–545. [[CrossRef](#)]

Disclaimer/Publisher’s Note: The statements, opinions and data contained in all publications are solely those of the individual author(s) and contributor(s) and not of MDPI and/or the editor(s). MDPI and/or the editor(s) disclaim responsibility for any injury to people or property resulting from any ideas, methods, instructions or products referred to in the content.